

Neural-MPC: Deep Learning Model Predictive Control for Quadrotors and Agile Robotic Platforms

Tim Salzmann¹, Elia Kaufmann², Marco Pavone³, Davide Scaramuzza² and Markus Ryll¹

Abstract—Model Predictive Control (MPC) has become a popular framework in embedded control for high-performance autonomous systems. However, to achieve good control performance using MPC, an accurate dynamics model is key. To maintain real-time operation, the dynamics models used on embedded systems have been limited to simple first-principle models, which substantially limits their representative power. In contrast to such simple models, machine learning approaches such as neural networks have been shown to accurately model even complex dynamic effects, but their large computational complexity hindered combination with fast real-time iteration loops. With this work, we present *Neural-MPC*, a framework to efficiently integrate large, complex neural network architectures as dynamics models within a model-predictive control pipeline. Our experiments, performed in simulation and the real world on a highly agile quadrotor platform, demonstrate up to 83% reduction in positional tracking error when compared to state-of-the-art MPC approaches without neural network dynamics.

I. INTRODUCTION

Model Predictive Control (MPC) has become one of the most popular frameworks in embedded control thanks to its ability of simultaneously address actuation constraints and performance objectives through optimization. Due to its predictive nature, the performance of MPC hinges on the availability of an accurate dynamics model of the underlying system. This requirement is exacerbated by strict real-time constraints, effectively limiting the choice of dynamics models on embedded platforms to simple first-principle models. Combining MPC with a more versatile and efficient dynamics model would allow an improvement in performance, safety and operation close to the robot’s physical limits.

Precise dynamics modeling of autonomous systems is challenging, e.g. when the platform approaches high speeds and accelerations or when in contact with the environment. Accurate modeling is especially challenging for autonomous aerial systems, as high speeds and accelerations can lead to complex aerodynamic effects [1], and operating in close proximity to obstacles with an aerial vehicle requires the modeling of interaction forces, e.g. ground effect. Data-driven approaches, in particular neural networks, have been shown to accurately model highly nonlinear dynamical effects. However, due to their large computational complexity, the integration of such models into embedded MPC pipelines remains challenging.

As a result, prior work on combining MPC with neural network-based dynamics [2], [3] was limited to applications

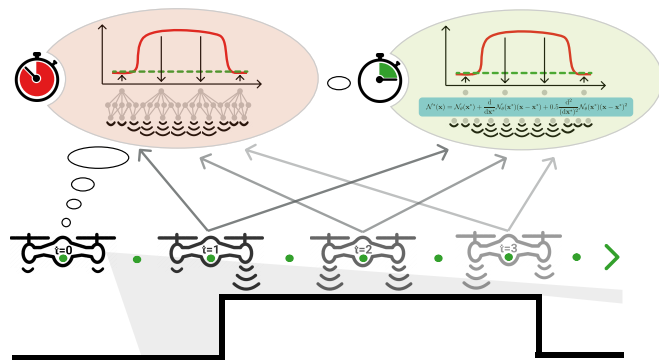


Fig. 1: Quadrotor Embedded Model Predictive Control modeling the ground effect by a neural network using a sensed height map as input. Naive integration of the neural network in the MPC optimization loop would lead to extensive optimization times (red). Our approach can handle complex deep learning models while being real-time capable, leveraging differential capabilities of modern machine learning frameworks and using approximations suitable for embedded agile platforms with fast dynamics (green).

with slow dynamics such as marine navigation [2] or chemical processes [3]. In contrast, for applications that feature fast dynamics, most prior work on data-driven control has focused on non-predictive control strategies [4], [5] or end-to-end controller learning [6]–[10]. While the former cannot account for actuation constraints, the latter require large datasets to train and do not allow for tuning without costly retraining.

A recent line of work proposes to combine learned dynamics represented by Gaussian Processes (GP) with MPC [11], [12]. By focusing on learning only an additive dynamics residual that is combined with a nominal model based on first principles, the learned model complexity can be reduced, enabling real-time operation. While demonstrating improved tracking performance compared to a nominal dynamics model, these approaches scale poorly to large datasets due to the nonparametric nature of GPs.

In this paper, we propose an efficient framework combining state-of-the-art Model Predictive Control with dynamics models represented by a deep neural network. The framework allows the integration of arbitrary neural network architectures as dynamics constraints into the MPC formulation by leveraging (GPU-)parallelized computation of Jacobians and Hessians provided by deep learning libraries such as PyTorch [13] and TensorFlow [14]. Compared to a plain integration of a deep network into an MPC framework, our approach allows unconstrained model selection and GPU acceleration, without measurable decrease in performance.

¹Tim Salzmann and Markus Ryll are with the Technical University of Munich {Tim.Salzmann, Markus.Ryll}@tum.de

²Elia Kaufmann and Davide Scaramuzza are with the University of Zurich {ekaufmann, sdavide}@ifi.uzh.ch

³Marco Pavone is with the Stanford University and NVIDIA Research pavone@stanford.edu

Our experiments, conducted with a highly agile quadrotor platform, show a substantial improvement in tracking performance. Quadrotors are a prime example of a robotic platform which benefits from an efficient and versatile dynamics model. Especially in agile flight maneuvers or maneuvers close to obstacles, their dynamics are hard to model accurately as complex aerodynamic forces start to dominate. We use such maneuvers to showcase the advantages of our approach while emphasizing that the proposed idea can easily be applied and benefit any controlled agile system such as autonomous vehicles or robotic arms.

Contribution

Our contribution is threefold: First, we formulate the computational paradigm for *Neural-MPC*, an MPC framework which uses deep learning models in the prediction step and can be scaled to large complex models while retaining real-time capability. Second, we describe and provide an open, extensible and free-to-use implementation of the *Neural-MPC* paradigm enabling other researchers to leverage (GPU-)parallelized automatic differentiation of modern machine learning frameworks for real-time MPC. Finally, we evaluate our approach on multiple simulation-based and real-world experiments using a high speed quadrotor in aggressive and close-to-obstacle maneuvers. To the best of the authors’ knowledge, this is the first approach capable of using powerful models, extending simple two layer networks, in a real-time embedded MPC setting; enabling scalability to large networks using modern machine learning concepts such as Convolutions.

II. RELATED WORK

With the advent of deep learning, there has been a considerable amount of research that aims to combine the representational capacity of deep neural networks with system modeling and control. In the following, we provide a brief overview of prior work that focuses on learning-based dynamics modeling, end-to-end controller learning, and the combination of data-driven dynamics models with traditional control pipelines.

Learned Dynamics Models. Thanks to their ability to identify patterns in large amounts of data, deep neural networks represent a promising approach to model complex dynamics. Previous works that leverage the representational power of deep networks for such modeling tasks include aerodynamics modeling of quadrotors [1], [15] and helicopters [16], turbulence prediction [17], tire friction modeling [18], and actuator modeling [19]. Although these works demonstrated that neural networks can learn system models that are able to learn the peculiarities of real-world robotic systems, they were restricted to simulation-only use cases or employed the network predictions as simple feedforward components in a traditional control pipeline.

Learned Controllers. With the rise of deep learning and especially deep reinforcement learning, a new class of controllers for robotic systems has emerged that directly maps sensory observations to actions. These controllers can either be trained in a supervised fashion by imitating actions of an expert controller [6], [7], [10] or by extensive interaction with a simulated environment [20]. As such, they do not

rely on online optimization and can potentially be combined with any dynamics model. Although such approaches achieve high control frequencies, they require large datasets to train, do not allow for tuning without costly retraining, and inevitably discard optimality, robustness and generalizability of the MPC framework, especially when deployed on out-of-distribution data.

Data-Driven Control. Leveraging the power of learned models in embedded control frameworks has been extensively researched in recent years. Most approaches have focused on combining the learned model with a simple reactive control scheme, such as the “Neural Lander” approach [4]. Neural Lander uses a learned model of the aerodynamic ground-effect to substantially improve a set-point controller in near-hover conditions. In [21], a learned recurrent dynamics model formulates a model-based control problem. While this approach allowed to adapt online to changing operating conditions, it cannot account for system constraints such as limited actuation input. Recent approaches that integrate the modeling strengths of data driven approaches in the MPC framework propose the use of Gaussian Processes as a learned residual model for race cars [12] and quadrotors [11]. For Gaussian Processes, both their complexity and accuracy scales with the number of inducing points and with their dimensionality. Embedded MPC often requires sampling times below 50ms leading to maximum of 10 inducing points for multidimensional problems [12] and 20 for unidimensional problems [11]. The pre-defined fixed kernel function in addition to the low number of feasible inducing points severely limit the performance of Gaussian Process MPC approaches. Instead of learning a residual model using GPs, [22] combines a sampling-based MPC with a dynamics model represented by a deep neural network. While this approach is successfully deployed on a miniature race car, the required sampling step limits its application to platforms with low-dimensional action space. In [23], a neural network dynamics model is combined with MPC for autonomous car racing, demonstrating high-performance driving at the friction limits of the tires. This approach uses the full network complexity in the optimizer, which requires the constraint of the network architecture to a simple two-layer models in order to maintain real-time operation.

Our work is inspired by [11], [12], [22], [23], but replaces the Gaussian Process dynamics of [11], [12] with deep neural networks and uses gradient-based optimization as opposed to a sampling-based scheme [22]. Compared to [23], we locally approximate the learned dynamics using a second-order Taylor approximation, which allows scaling the learned dynamics model beyond simple two-layer MLPs without compromising accuracy. The resulting framework allows combination of the versatile modeling capabilities of deep neural networks with state-of-the-art embedded optimization software without tightly constraining the choice of network architecture.

III. NEURAL MODEL PREDICTIVE CONTROL

In its most general form, MPC finds an optimal input command \mathbf{u} associated with a cost function \mathcal{L} subject to its system dynamics model $\dot{\mathbf{x}} = f(\mathbf{x}, \mathbf{u})$ along a reference $\mathbf{x}_r(t)$, $\mathbf{u}_r(t)$. As such, MPC has the distinctive capacity to account

for constraints on input and state variables for current and future timesteps in its control output. Traditionally, the model f is defined using "simple" first principles \mathcal{F} to be real-time capable (Fig. 2(a)). This definition can be extended such that f can be a mathematical combination of first principles \mathcal{F} and one or multiple data driven models \mathcal{D} . This enables more general models extending the capability of first principles.

$$\begin{aligned} \min_{\mathbf{u}} \int \mathcal{L}(\mathbf{x}, \mathbf{u}) \\ \text{subject to} \quad & \mathbf{x}(t_0) = \mathbf{x}_0 \\ & \dot{\mathbf{x}} = f_{\mathcal{F}}(\mathbf{x}, \mathbf{u}) + f_{\mathcal{D}}(\mathbf{x}, \mathbf{u}) \\ & \mathbf{r}(\mathbf{x}, \mathbf{u}) \leq 0 \end{aligned} \quad (1)$$

where \mathbf{x}_0 denotes the initial condition and \mathbf{r} can incorporate (in-)equality constraints, such as bounds in state and input variables. In practice, the system is typically discretized into N steps over a time horizon T and optimized using sequential quadratic programming (SQP).

Traditionally, learned dynamics models fall into different conceptual categories (Fig. 2) with regards to modeling capacity and real-time capability:

- Fig. 2(b) - Using complex and computationally demanding first-principle formulations rejecting real-time capabilities and thus, becoming infeasible for real-world application [24].
- Fig. 2(c) - Using simplistic data driven models (e.g. 1D Gaussian Process with small number of supporting vectors) [11].
- Fig. 2(d) - Using large data-driven models, only feasible for simulation purposes [1].

The target, however, is a framework capable of modeling complex high-dimensional dynamics while being computationally cheap for real time capability - Fig. 2(e).

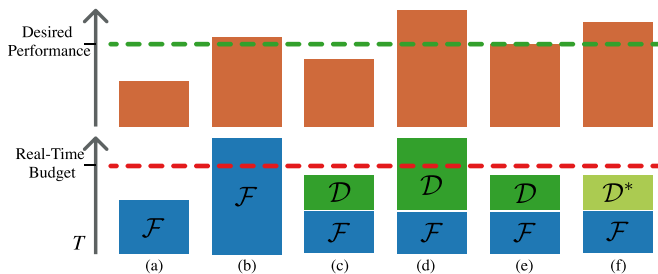


Fig. 2: Conceptual overview of data driven MPC approaches compared by their performance and real-time capability. (a) Simple first principle model. (b) Complex first principle model. (c) First principle model with small data-driven residual. (d) First principle model with large data-driven residual. (e) First principle model with small data-driven residual model but sufficient in performance used in the *full integration* scheme. (f) First principle model with adapted data-driven residual model such as in our *distributed integration* scheme.

A. Neural-MPC - A Computational Paradigm

We describe a twofold procedure enabling the integration of neural networks into MPC. Depending on the complexity

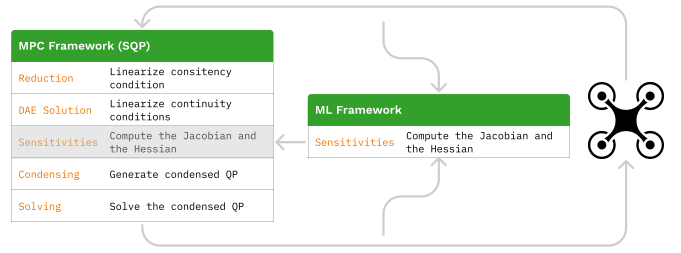


Fig. 3: Data flow for our distributed integration. The sensitivities calculation of the learned model parts is performed by the Machine Learning framework instead of the SQP. A detailed explanation of the individual SQP steps can be found in [27].

of the network to be integrated, our framework allows either *full* integration for simple architectures (Fig. 2(e)) or *distributed* integration for complex models (Fig. 2(f)) which would otherwise not be real-time capable.

Full Integration. For applications where the desired performance increase by the neural network can be achieved with a small multilayer perceptron network such that the plain integration of the learned model $f_{\mathcal{D}}$ is real-time capable in an MPC framework, we use the full trained network in the optimization loop. In this case the first and possibly second order sensitivities (Jacobian and Hessian) of the dynamics function have to be calculated by the SQP algorithm to feed the underlying quadratic programming (QP) solver.

Distributed Integration. Sensitivity analyses and model simulation are part of the most expensive steps in SQP schemes [25], scaling with the complexity of the model. As MPC models traditionally rely on first order principles, state-of-the-art frameworks for MPC (e.g. CasADi [26]) are optimized to evaluate those and calculate their sensitivities efficiently. In contrast, they are not optimized for models consisting mainly of (large) matrix multiplications such as neural network approaches. For these, however, there are frameworks such as PyTorch [13] and TensorFlow [14] which specialize in efficient training, evaluation, and — most importantly — gradient calculation of deep learning models. To leverage this strength we *distribute* the simulation and sensitivity analysis of the learned model $f_{\mathcal{D}}$ to the respective machine learning framework, enabling the possibility to use GPU acceleration, and forward the results to the MPC framework to be used in the QP solver. This procedure is visualized in Fig. 3. As such we are not limited by the modeling language of the MPC framework but can rather leverage the entire modeling power of modern machine learning frameworks.

Note, that the results of both integration schemes are numerically identical while they differ in optimization time.

B. Neural-MPC - Implementation

To demonstrate the applicability of the Neural-MPC paradigm, we implement it using CasADi [26] and PyTorch [13] as the MPC and ML framework respectively. CasADi is a software tool commonly used for non-linear optimization and automatic differentiation in robotic control applications. The key feature of CasADi, making it viable for embedded real-time problems, is its ability to generate

native C code for model evaluation and differentiation.

While a scheme similar to the *full integration* was implemented using CasADi and put to use in the past by [23], no openly accessible implementation was provided. In contrast, while realizing the *full integration*, we provide the research community with an open and extensible modeling language, mirroring PyTorch syntax, creating both PyTorch and CasADi computational graphs internally. The PyTorch graph can be used to leverage its extensive ecosystem for training machine learning models. The CasADi graph can be, combined with further CasADi-based operations, used in an optimization problem, including code generation. To create both graphs in parallel, the modeled mathematical operations are fixed by the intersection of operations between PyTorch and CasADi. We enable the research community to create simple deep learning models, such as applied in [23] (2 layers = 1 hidden layer with 64 neurons), trainable in PyTorch and usable in a CasADi optimization as easy as:

```
import ml_casadi.torch as mc
mlp_nn = mc.MultiLayerPerceptron(
    input_size=6,
    hidden_size=64,
    output_size=3,
    n_hidden=1,
    activation='tanh')
y_t: torch.Tensor = mlp_nn(x: torch.Tensor)
y_c: cs.MX = mlp_nn(x: cs.MX)
```

In the proposed MPC setting we define such a full, double headed PyTorch/CasADi graph for the learned data-driven components of the dynamics model f_D and combine it with first principle model f_F also modeled in CasADi.

Unfortunately, implementing the *distributed integration* paradigm directly as described is currently infeasible, as it would require extensive adaptation of CasADi to support the external calculation of sensitivities from CasADi to PyTorch. This would involve integrating PyTorch's C++ library into CasADi and its code generation routine; which is left as future work. However, we provide an implementation which approximates the *distributed integration* closely, such that for our task, agile embedded systems with high control frequencies, suffer no performance decrease by this approximation in practice.

To give the interested reader a deep understanding we describe the procedure in detail: We represent the neural network dynamics model f_D by a Taylor Approximation of up to second degree around approximation point \mathbf{a}^* .

$$f_D^*(\mathbf{a}) = f_D^{\mathbf{a}^*} + \mathbf{J}_D^{\mathbf{a}^*}(\mathbf{a} - \mathbf{a}^*) + 0.5 \mathbf{H}_D^{\mathbf{a}^*}(\mathbf{a} - \mathbf{a}^*)^2 \quad (2)$$

where $\mathbf{a} = [\mathbf{x}, \mathbf{u}]$ This approximation is modeled as a CasADi graph, leaving model output at the approximation point $f_D^{\mathbf{a}^*}$, the Jacobian $\mathbf{J}_D^{\mathbf{a}^*}$, and the Hessian $\mathbf{H}_D^{\mathbf{a}^*}$ as symbolic parameters. The resulting CasADi model f_D^* is combined with possible first principle approaches f_F to result in the full dynamics equation represented in CasADi. During optimization, after each SQP solution, we efficiently re-compute the PyTorch model's evaluation and sensitivity results, using PyTorch's (GPU)-parallelized automatic differentiation engine. Here, the previous optimization result at

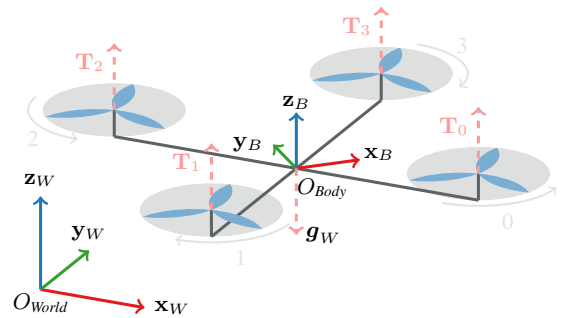


Fig. 4: Quadrotor model with world and body frames and propeller numbering convention. Grey arrows indicate the spinning direction of the individual rotors.

all horizon steps \mathbf{x}'_k and \mathbf{u}'_k serve as set-points. The resulting evaluation and differentiation values $f_D^{\mathbf{x}'_k, \mathbf{u}'_k}$, $\mathbf{J}_D^{\mathbf{x}'_k, \mathbf{u}'_k}$ and $\mathbf{H}_D^{\mathbf{x}'_k, \mathbf{u}'_k}$ are used to define the respective symbolic parameters in the CasADi function in the next SQP optimization.

Notably, we are able to calculate the sensitivities at all horizon steps in a single batch leading to lower optimization times. It is easy to show that for a (Gauss-)Newton's method the error induced by this approximation is only in the second order of the perturbation $\epsilon = [\mathbf{x}'_k, \mathbf{u}'_k] - [\mathbf{x}_k, \mathbf{u}_k]$ and, as we are specifically tackling embedded real-time application with high frequency control schemes, we can assume small ϵ for subsequent optimization cycles. This adapted procedure leads to a small constant overhead as CasADi internally has to re-compute the sensitivities of the Taylor approximation.

Because a sub-optimal timely input command is preferred over an optimal late one, embedded MPC applications subjected to fast dynamics are commonly solved with the real-time-iteration scheme (RTI) [27], where only a single SQP iteration is executed. In this case the solution by the implemented *distributed integration* is numerically identical with the solution of the *full integration* as only a single Quadratic Program is solved. This can be seen in Section V where both approaches perform equally well in predictive power while differing in run-time using RTI-MPC.

The described CasADi integration can be used in MPC, both with a SQP defined in CasADi or acados [25], which provides additional routines for fast and embedded nonlinear optimal control relying on a CasADi dynamics model.

IV. METHODOLOGY

While the idea described in Section III can be applied to a variety of robotic applications, we will use agile quadrotor flight maneuvers to showcase its potential.

A. Notation

Scalars are denoted in lowercase s , vectors in lowercase bold \mathbf{v} , and matrices in uppercase bold \mathbf{M} . Coordinate frames such as the World W and Body B frames are defined with orthonormal basis i.e. $\{\mathbf{x}_W, \mathbf{y}_W, \mathbf{z}_W\}$, with the Body frame being located at the center of mass of the quadrotor (see Fig. 4).

A vector from coordinate p_1 to p_2 expressed in the W frame is written as ${}_W \mathbf{v}_{12}$. If the vector's origin coincides with the frame it is described in, the frame index is dropped, e.g.

the quadrotor position is denoted as \mathbf{p}_{WB} . Orientations are represented using unit quaternions $\mathbf{q} = (q_w, q_x, q_y, q_z)$ with $\|\mathbf{q}\| = 1$, such as the attitude state of the quadrotor body \mathbf{q}_{WB} . Finally, full SE3 transformations, such as changing the frame of reference from Body to World for a point \mathbf{p}_{B1} , are described by ${}^W\mathbf{p}_{B1} = {}^W\mathbf{t}_{WB} + \mathbf{q}_{WB} \odot \mathbf{p}_{B1}$. Note the quaternion-vector product denoted by \odot representing a rotation of the vector \mathbf{v} by the quaternion \mathbf{q} as in $\mathbf{q} \odot \mathbf{v} = \mathbf{q}\mathbf{v}\bar{\mathbf{q}}$, where $\bar{\mathbf{q}}$ is the quaternion's conjugate.

B. Nominal Quadrotor Dynamics Model

The nominal dynamics assume the quadrotor to be a 6 degree-of-freedom rigid body of mass m and diagonal moment of inertia matrix $\mathbf{J} = \text{diag}(J_x, J_y, J_z)$. Our model is similar to [11], [28], [29] as we write the nominal dynamics $\dot{\mathbf{x}}$ up to second order derivatives, leaving the quadrotors individual rotor thrusts $T_i \forall i \in (0, 3)$ as control inputs $\mathbf{u} \in \mathbb{R}^4$. The state space is thus 13-dimensional and its dynamics can be written as:

$$\dot{\mathbf{x}} = \begin{bmatrix} \dot{\mathbf{p}}_{WB} \\ \dot{\mathbf{q}}_{WB} \\ \dot{\mathbf{v}}_{WB} \\ \dot{\boldsymbol{\omega}}_B \end{bmatrix} = \mathbf{f}_{\mathcal{F}}(\mathbf{x}, \mathbf{u}) = \begin{bmatrix} \mathbf{v}^W \\ \mathbf{q}_{WB} \cdot \begin{bmatrix} 0 \\ \boldsymbol{\omega}_B/2 \end{bmatrix} \\ \frac{1}{J} \mathbf{q}_{WB} \odot \mathbf{T}_B + \mathbf{g}_W \\ \mathbf{J}^{-1} (\boldsymbol{\tau}_B - \boldsymbol{\omega}_B \times \mathbf{J} \boldsymbol{\omega}_B) \end{bmatrix}, \quad (3)$$

with $\mathbf{g}_W = [0, 0, -9.81 \text{ m/s}^2]^\top$ denoting Earth's gravity, \mathbf{T}_B the collective thrust and $\boldsymbol{\tau}_B$ the body torque as in:

$$\mathbf{T}_B = \begin{bmatrix} 0 \\ 0 \\ \sum T_i \end{bmatrix} \quad \text{and} \quad \boldsymbol{\tau}_B = \begin{bmatrix} d_y(-T_0 - T_1 + T_2 + T_3) \\ d_x(-T_0 + T_1 + T_2 - T_3) \\ c_\tau(-T_0 + T_1 - T_2 + T_3) \end{bmatrix}.$$

The horizontal displacements d_x, d_y are measured between each motor and the center of gravity of the platform. The rotor's drag torque constant is denoted by c_τ . We use an explicit Runge-Kutta method of 4th order $\mathbf{f}^{RK4}(\mathbf{x}, \mathbf{u})$ to integrate $\dot{\mathbf{x}}$ given an initial state \mathbf{x}_k , input \mathbf{u}_k and integration step δt by:

$$\mathbf{x}_{k+1} = \mathbf{f}_{\mathcal{F}}^{RK4}(\mathbf{x}_k, \mathbf{u}_k, \delta t).$$

C. Augmented Aerodynamic Residual Models

Following previous works [11], [12], we use the data driven model, in the form of a neural network \mathcal{N} , to complement the nominal dynamics by modeling a residual. In its full configuration, our residual dynamics model is defined as

$$\mathbf{f}_{\text{dyn}}(\mathbf{x}, \mathbf{u}) = \mathbf{f}_{\mathcal{F}}(\mathbf{x}, \mathbf{u}) + \mathbf{f}_{\mathcal{D}}(\mathbf{x}, \mathbf{u}), \quad (4)$$

$$\mathbf{f}_{\mathcal{D}}(\mathbf{x}, \mathbf{u}) = \begin{bmatrix} \mathbf{0}_2 \\ \mathbf{f}_{\mathcal{D}_\theta}(\mathbf{x}, \mathbf{u}) \\ \mathbf{f}_{\mathcal{D}_\psi}(\mathbf{x}, \mathbf{u}) \end{bmatrix},$$

where we individually account for disturbances in linear and angular accelerations unknown to the nominal dynamics and θ and ψ are the parameters of the neural networks modeling linear and angular disturbances respectively.

We also evaluate two slimmed down versions of the residual model

$$\mathbf{f}_{\mathcal{D}_a}(\mathbf{x}, \mathbf{u}) = \begin{bmatrix} \mathbf{0}_2 \\ \mathbf{f}_{\mathcal{D}_\theta}(\mathbf{v}_B) \\ 0 \end{bmatrix}, \quad \mathbf{f}_{\mathcal{D}_{a,u}}(\mathbf{x}, \mathbf{u}) = \begin{bmatrix} \mathbf{0}_2 \\ \mathbf{f}_{\mathcal{D}_\theta}(\mathbf{v}_B, \mathbf{u}) \\ 0 \end{bmatrix}. \quad (5)$$

D. Augmented Ground Effect Model

To show the strength of our approach, leveraging a complex arbitrary high level input, we extend the residual model using a height map under the quadrotor as additional input to model the ground effect.

$$\mathbf{f}_{\mathcal{D}_g}(\mathbf{x}, \mathbf{u}) = \begin{bmatrix} \mathbf{0}_2 \\ \mathbf{f}_{\mathcal{N}_\theta}(\mathbf{x}, \mathbf{u}, z_{WB} - h_l(\mathbf{p}_{WB}, \mathbf{H}_W)) \\ 0 \end{bmatrix}$$

where z_{WB} is the altitude of the quadrotor and h_l is a mapping $h_l : \mathbb{R}^3 \times \mathbb{R}^{N \times M} \rightarrow \mathbb{R}^{3 \times 3}$ which takes the quadrotor's position \mathbf{p}_{WB} and a fixed or sensed global height map \mathbf{H}_W of size $N \times M$ as input. The function returns a 3×3 local patch of the height map around the quadrotor's position with a resolution of 10 cm.

E. MPC Cost Formulation

We specify the cost in Eq. (1) to be of quadratic form $\mathcal{L}(\mathbf{x}, \mathbf{u}) = \|\mathbf{x} - \mathbf{x}_r\|_Q^2 + \|\mathbf{u} - \mathbf{u}_r\|_R^2$ and discretize the system into N steps over time horizon T of size $dt = T/N$. We account for input limitations by constraining $0 \leq \mathbf{u} \leq u_{\max}$, and optionally include the predictions by the data driven model within the system dynamics.

$$\min_{\mathbf{u}} \mathbf{x}_N^\top Q \mathbf{x}_N + \sum_{k=0}^N \mathbf{x}_k^\top Q \mathbf{x}_k + \mathbf{u}_k^\top R \mathbf{u}_k$$

subject to $\mathbf{x}_{k+1} = \mathbf{f}_{\text{dyn}}^{RK4}(\mathbf{x}_k, \mathbf{u}_k, \delta t)$

$$\mathbf{x}_0 = \mathbf{x}_{\text{init}}$$

$$u_{\min} \leq \mathbf{u}_k \leq u_{\max}$$

where $\mathbf{f}_{\text{dyn}}^{RK4}$ can be extended with one of the residual dynamics $\mathbf{f}_{\mathcal{D}_*}^{RK4}$.

The optimization problem is solved by constructing a multiple shooting scheme and using a sequential quadratic programming (SQP), leveraging Gauss-Newton approximation in a real-time iteration (RTI) scheme [27]. The optimization problem is implemented using acados [25].

V. EXPERIMENTS

Our experiments are structured to show the usefulness, performance and real-time capability of our approach. The experimental setup is based on agile high-speed trajectory tracking and is extended with additional experiments on close-proximity flight.

All our experiments are divided in two phases: system identification and evaluation. During system identification, we collect data using the nominal dynamics model in the MPC controller. During evaluation we track two fixed evaluation trajectories, Circle and Lemniscate, and rate the performance based on the reference position tracking error. As such, we report the (Mean) Euclidean Distance between the reference trajectory and the tracked trajectory as error.

To identify model architectures used in the experiments we use a naming convention stating the model type followed by the size and the integration scheme (for neural network model only). GP-20 is a Gaussian Process Model with 20 inducing points while N-3-32-D is a neural network model with 3 hidden layers, 32 neurons each using the *distributed integration* scheme.

TABLE I: Results for the Simplified Simulation experiment. Our deep learning models outperform Gaussian Processes even using small models. For large models our *distributed integration* allows real-time capability without performance decrease compared to the *full integration*.

Track	Error [mm]															t [ms] avg
	Random					Circle					Lemniscate					
v_{avg} [m/s]	2	2.7	3	3.2	3.5	2	4.5	7	9.5	12	2	4.5	7	9.5	12	avg
v_{max} [m/s]	7.0	9.6	10.5	11.2	12.3	2.1	4.8	7.5	10.2	12.8	2.9	5.9	10.5	14.0	18.1	avg
Perfect	1	4	7	9	12	1	0	1	1	2	0	1	3	11	28	1.0
Nominal	113	146	157	162	174	50	134	213	277	333	50	124	187	244	297	1.0
GP-20	35	38	37	36	35	22	31	28	29	35	34	33	35	33	50	2.9
GP-50	35	39	40	42	42	23	37	39	42	40	27	37	39	41	52	4.5
GP-100	21	23	24	26	28	21	20	26	31	30	19	21	25	27	44	7.2
N-1-12-F	37	38	38	38	38	33	33	35	34	33	28	32	33	32	48	1.6
N-2-18-F	24	28	29	29	32	21	22	27	31	30	19	23	27	30	43	2.7
N-3-32-F	16	19	25	26	27	13	17	22	27	26	14	19	26	28	45	8.2
N-3-32-D	16	19	24	26	26	13	17	22	27	26	14	19	26	28	46	2.2
N-4-64-F	12	16	20	24	26	10	14	18	23	23	11	17	27	27	45	35.9
N-4-64-D	12	16	20	24	26	10	14	17	22	23	11	17	27	27	46	2.3
N-5-128-F	15	22	25	27	31	13	18	22	28	29	16	19	31	29	47	178.7
N-5-128-D	16	22	25	27	31	13	18	22	28	29	16	19	31	29	49	3.2

A. Simulation

We use two simulation environments featuring varying modeling accuracy and real-time requirements to compare our approach against a non-augmented MPC controller as well as [11] with respect to real-time capability and model capacity.

Simplified Quadrotor Simulation. We use the simulation framework described in [11], where perfect odometry measurements and ideal tracking of the commanded single rotor thrusts are assumed. Drag effects by the rotors and fuselage are simulated, as well as zero mean ($\sigma = 0.005$) constant Gaussian noise on forces and torques, and zero mean Gaussian noise on motor voltage signals with standard deviation proportional to the input magnitude $\sigma = 0.02\sqrt{u}$. There are no run-time constraints as controller and simulator are run sequentially in simulated time. Using the simplified simulation we analyze the predictive performance and runtime of our Neural-MPC for varying network sizes and directly compare to the Gaussian Process approach. We constrain the residual model to linear accelerations $\mathbf{f}_{\mathcal{F}_a}$ to facilitate comparison with prior work [11]. To evaluate the run-times of our full and distributed approach fairly and considering the limited resources of embedded systems this experiment was performed on a single CPU core.

The results obtained in the simplified simulation setting are depicted in Table I. In addition to Gaussian Processes, we compare with a *Nominal* model where no learned residuals are modeled in the dynamics function and we also compare with an oracle-like *Perfect* model which uses the same dynamics equations as the simulation (excluding noise). Our approach outperforms Gaussian Processes [11] on all tested trajectories. Even small models (N-1-12-F), which are integrated in full in the MPC, perform on par with GP's performance using 50 inducing points. Larger models further improve performance while being real-time capable when integrated using our distributed approach. Small differences in the results between our *full* and *distributed integration* in the RTI setting are due to random noise modeled in the simulation.

BEM Quadrotor Simulation. In addition to the simplified

TABLE II: Results for the BEM Simulation experiment. Adding extra input dimensions improves tracking performance but brings GPs to the computational limit. Our approach can leverage multidimensional inputs while being real-time capable. Differences in optimization time compared to Table I result from python's Global Interpreter Lock (GIL) confining optimization and ROS (callback) threads to the same physical core.

Dynamic Conf.	Track	Error [mm]			t [ms]
		Circle	Lemniscate	avg	
		v_{max} [m/s]	10	14	avg
	Nominal		245	225	1.2
Eq. (3) $\mathbf{f}_{\mathcal{F}}$	GP-20	81	69	3.9	
	GP-50	57	70	5.3	
	GP-100	60	61	7.8	
	N-3-32-F	50	59	7.2	
	N-3-32-D	50	61	3.2	
Eq. (5) $\mathbf{f}_{\mathcal{D}_a}$	N-4-64-F	60	70	19.5	
	N-4-64-D	50	59	3.4	
	GP-20	61	67	8.1	
	GP-50	64	57	14.4	
Eq. (5) $\mathbf{f}_{\mathcal{D}_{a,u}}$	GP-100	69	67	19.2	
	N-3-32-F	30	50	8.4	
	N-3-32-D	30	52	3.3	
	N-4-64-D	31	52	3.4	
	Eq. (4) $\mathbf{f}_{\mathcal{D}}$	N-3-32-D	12	38	4.2
N-4-64-D		13	38	5.0	

simulation setting, we also evaluate our approach in a highly accurate aerodynamics simulator based on Blade-Element-Momentum-Theory (BEM) [1]. In contrast to the simplified simulation setting, this simulation can accurately model lift and drag produced by each rotor from the current ego-motion of the platform and the individual rotor speeds. The simulator runs in real time and communicates with the controller via the Robot Operating System (ROS). We target a real-time control frequency of 100 Hz.

The results obtained in this simulation setting are illustrated in Table II. When modeling only the velocity dependent aerodynamic residuals $\mathbf{f}_{\mathcal{F}_a}$ we outperform GPs. Large models (N-4-64) overshoot the real-time budget of 10 ms in the *full integration* scheme, leading to inferior performance. The same model using our (distributed integration) scheme is real-time capable with good performance. The maximum tracking performance, however, is limited as the simulated linear accelerations by the BEM model are dependent on the rotor speeds. As rotor speeds and thrusts are connected by a bijective function this influence can be learned by our model by supplying the rotor thrusts as additional input $\mathbf{f}_{\mathcal{F}_{a,u}}$. When we add thrust input to the Gaussian Processes we can see an improvement for the GP-20 model. For GP models with more inducing points the increased input dimension (from 1 to 5) slows down the posterior kernel vector calculation, bringing the optimization time above our real-time budget and negatively impacting performance. By contrast, our approach can make full use of the additional information and substantially improves performance. Finally, we evaluate the full residual model $\mathbf{f}_{\mathcal{D}}$ modeling linear and rotational acceleration disturbances. This becomes infeasible for GPs from a run-time perspective. Using our approach, predicting the full disturbances ultimately improves the tracking performance by up to 95% compared to the nominal model. Differences in performance between the *full* and *distributed* scheme result from timing differences in optimization and communication via ROS between the controller and the

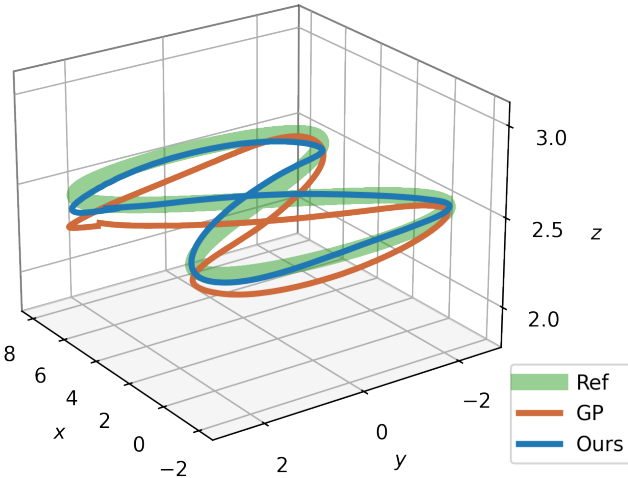


Fig. 5: Illustration of the lemniscate trajectory executed in the real world experiments. While our approach stays close to the reference trajectory, the positional tracking error of the GP is higher.

simulator. The lower theoretical performance bound is set by contrasting discretization and integration schemes between controller and simulator and communication delays in ROS.

B. Real World

Finally, we perform real world experiments evaluating our approach by performing a set of agile trajectories using a physical quadrotor platform. This quadrotor features a thrust-to-weight ratio of 5:1 and weighs 0.8kg. Control commands in the form of desired collective thrust and body rates are computed on a laptop at 100 Hz and sent to the quadrotor wireless. These commands are then tracked by an onboard PID controller. All real-world flight experiments are performed in an instrumented tracking arena that provides accurate pose estimates at 400 Hz. As in the simulation experiments, we compare the tracking error along both circle and lemniscate trajectories at speeds up to 14 ms^{-1} . Following [11] we train GP and Neural-MPC models on the circle and lemniscate trajectories and evaluate them in all permutations. We evaluate our approach against the nominal controller and the Gaussian Process configuration deployed in [11]. The results of these experiments can be seen in Table III, where we improve positional tracking error by up to 83% compared to the nominal controller. Further, we consistently outperform Gaussian Processes by up to 57%. A comparison of our approach compared to a GP is visualized in Fig. 5.

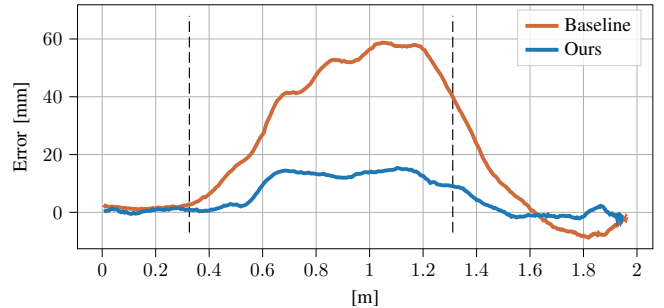
Ground Effect. Finally, we evaluate the capability of our model (Section IV-D), modeling the complex aerodynamics of the ground effect using a height map as input. We place a table of 70 cm height in the flight arena and collect data by repeatedly flying over the table in close proximity. Note that in order to collect data in very close proximity to the table, the tracking reference during data collection had to be set below the table’s surface to compensate for the ground effect during data collection. During evaluation, we fly repeated trajectories over the table with a target altitude of 80 cm of the quadrotor’s center of gravity; leaving

TABLE III: Results for the Real-World experiment. We improve tracking performance up to 83% compared to the nominal controller and up to 57% compared to GPs.

Track	Error [mm]			
	Circle		Lemniscate	
Trained on	Circle	Lemniscate	Circle	Lemniscate
v_{\max} [m/s]	10	14	10	14
Eq. (3) $f_{\mathcal{F}}$: Nominal	321		359	
Eq. (5) $f_{\mathcal{D}_a}$: GP-20	67	209	115	265
Eq. (5) $f_{\mathcal{D}_a}$: N-3-32	53	201	98	134
Eq. (4) $f_{\mathcal{D}_a}$: N-3-32	57	193	108	115



(a)



(b)

Fig. 6: (a) Depiction of the Quadrotor overflying the table in close proximity to the plane. (b) Visualization of our approach modeling the aerodynamic effects close to the table. Vertical lines mark the positions of the quadrotor being over the table with any part of its body and leaving the table’s plane. Our approach can model the aerodynamic effects in close proximity to the ground, substantially limiting the linear tracking error in z .

approximately 2 cm between the table and the lowest point of the quadrotor (battery). To isolate the performance of our approach, compensating for ground effect, we evaluate the trained model in two configurations. First, in which the height map information is unknown to the model (Baseline), and second where the information is known to the model. On an evaluation trajectory with 8 flyovers we improve the tracking error in z direction by 72% in close proximity (table plane +10 cm in xy) above of the table. A visualization of a single flyover can be seen in Fig. 6. We want to point out that the controller penalizes deviations in control compared to the calculated reference (using nominal dynamics) in order to avoid extreme control commands. This limits the controller to fully adapt to the modeled ground effect by the neural network, leading to an ultimately higher error compared to the raw performance of the network. This could be improved

by limiting command fluctuations in a different way, for example by defining limits on control derivatives.

VI. CONCLUSION

In this work we demonstrated an alternative approach to existing data-driven MPC frameworks. We outperform them in simplicity, performance, modeling capability, and application diversity. The modeling capabilities of the Neural-MPC are merely limited by the underlying Machine Learning framework, while the run-time is kept down using our *distributed integration*; making our approach generalizable to a variety of control applications.

In the real world, our approach is limited by the ability to perform an accurate system identification on the real hardware. Factors such as communication delays, physical time constants and noise have to be considered to create a dataset usable for training the data-driven models. Research advances in accurate system identification will have a direct impact on the real-world performance of Neural-MPC. Further, Gaussian Processes bring the advantages of implicitly modeling the posterior uncertainty. This can, for example, be useful in MPC approaches to include chance constraints on the boundaries. Neural networks by default do not have this implicit notion in uncertainty but can learn to predict the parameters of a distribution as output in addition to the mean only. We leave this as future work.

The possibility to accurately model highly complex dynamics in an MPC framework also enables new applications and use cases for quadrotors in the future. As such, we want to explore the possibility to optimize a quadrotor's trajectory for efficiency, leveraging the learned ground effect. Further, we want to explore the possibility to learn residual models online while flying.

REFERENCES

- [1] L. Bauersfeld, E. Kaufmann, P. Foehn, S. Sun, and D. Scaramuzza, "NeuroBEM: Hybrid Aerodynamic Quadrotor Model," in *Robotics: Science and Systems*, 2021.
- [2] C. Liu, C. Li, and W. Li, "Computationally efficient MPC for path following of underactuated marine vessels using projection neural network," *Neural Computing and Applications*, 2020.
- [3] P. Kittisupakorn, P. Thitiyasook, M. Hussain, and W. Daosud, "Neural network based model predictive control for a steel pickling process," *Journal of Process Control*, 2009.
- [4] G. Shi, X. Shi, M. O'Connell, R. Yu, K. Azzadenesheli, A. Anandkumar, Y. Yue, and S.-J. Chung, "Neural Lander: Stable Drone Landing Control using Learned Dynamics," in *Int. Conf. on Robotics and Automation (ICRA)*, 2019.
- [5] M. Faessler, A. Franchi, and D. Scaramuzza, "Differential flatness of quadrotor dynamics subject to rotor drag for accurate tracking of high-speed trajectories," *IEEE Robotics and Automation Letters*, 2017.
- [6] E. Maddalena, C. da S. Moraes, G. Waltrich, and C. Jones, "A Neural Network Architecture to Learn Explicit MPC Controllers from Data," *IFAC-PapersOnLine*, 2020.
- [7] J. Nubert, J. Köhler, V. Berenz, F. Allgöwer, and S. Trimpe, "Safe and Fast Tracking on a Robot Manipulator: Robust MPC and Neural Network Control," *IEEE Robotics and Automation Letters*, 2020.
- [8] D. Wang, Z. J. Shen, X. Yin, S. Tang, X. Liu, C. Zhang, J. Wang, J. Rodriguez, and M. Norambuena, "Model Predictive Control Using Artificial Neural Network for Power Converters," *IEEE Trans. on Industrial Electronics*, 2022.
- [9] R. Winqvist, A. Venkitaraman, and B. Wahlberg, "On Training and Evaluation of Neural Network Approaches for Model Predictive Control," in *arXiv preprint*, 2020.
- [10] E. Kaufmann, A. Loquercio, R. Ranftl, M. Müller, V. Koltun, and D. Scaramuzza, "Deep drone acrobatics," *RSS: Robotics, Science, and Systems*, 2020.
- [11] G. Torrente, E. Kaufmann, P. Foehn, and D. Scaramuzza, "Data-Driven MPC for Quadrotors," in *IEEE Robotics and Automation Letters*, 2021.
- [12] J. Kabzan, L. Hewing, A. Liniger, and M. N. Zeilinger, "Learning-Based Model Predictive Control for Autonomous Racing," *IEEE Robotics and Automation Letters*, 2019.
- [13] A. Paszke, S. Gross, F. Massa, A. Lerer, J. Bradbury, G. Chanan, T. Killeen, Z. Lin, N. Gimelshein, L. Antiga, A. Desmaison, A. Köpf, E. Yang, Z. DeVito, M. Raison, A. Tejani, S. Chilamkurthy, B. Steiner, L. Fang, J. Bai, and S. Chintala, "PyTorch: An Imperative Style, High-Performance Deep Learning Library," *Advances in Neural Information Processing Systems*, 2019.
- [14] M. Abadi, A. Agarwal, P. Barham, E. Brevdo, Z. Chen, C. Citro, G. S. Corrado, A. Davis, J. Dean, M. Devin, S. Ghemawat, I. Goodfellow, A. Harp, G. Irving, M. Isard, Y. Jia, R. Jozefowicz, L. Kaiser, M. Kudlur, J. Levenberg, D. Mane, R. Monga, S. Moore, D. Murray, C. Olah, M. Schuster, J. Shlens, B. Steiner, I. Sutskever, K. Talwar, P. Tucker, V. Vanhoucke, V. Vasudevan, F. Viegas, O. Vinyals, P. Warden, M. Wattenberg, M. Wicke, Y. Yu, and X. Zheng, "TensorFlow: Large-Scale Machine Learning on Heterogeneous Distributed Systems," 2016.
- [15] S. Bansal, A. K. Akametalu, F. J. Jiang, F. Laine, and C. J. Tomlin, "Learning quadrotor dynamics using neural network for flight control," in *IEEE Conf. on Decision and Control*, 2016.
- [16] A. Punjani and P. Abbeel, "Deep learning helicopter dynamics models," in *IEEE Int. Conf. on Robotics and Automation (ICRA)*, 2015.
- [17] Z. Li, N. B. Kovachki, K. Azzadenesheli, K. Bhattacharya, A. Stuart, and A. Anandkumar, "Fourier neural operator for parametric partial differential equations," in *Int. Conf. on Learning Representations*, 2020.
- [18] N. A. Spielberg, M. Brown, N. R. Kapania, J. C. Kegelmann, and J. C. Gerdes, "Neural network vehicle models for high-performance automated driving," *Science Robotics*, 2019.
- [19] J. Hwangbo, J. Lee, A. Dosovitskiy, D. Bellicoso, V. Tsounis, V. Koltun, and M. Hutter, "Learning agile and dynamic motor skills for legged robots," *Science Robotics*, 2019.
- [20] O. M. Andrychowicz, B. Baker, M. Chociej, R. Jozefowicz, B. McGrew, J. Pachocki, A. Petron, M. Plappert, G. Powell, and A. Ray, "Learning dexterous in-hand manipulation," *Int. J. Robot. Research*, 2020.
- [21] I. Lenz, R. Knepper, and A. Saxena, "DeepMPC: Learning Deep Latent Features for Model Predictive Control," in *Robotics: Science and Systems*, 2015.
- [22] G. Williams, N. Wagener, B. Goldfain, P. Drews, J. M. Rehg, B. Boots, and E. A. Theodorou, "Information theoretic MPC for model-based reinforcement learning," in *2017 IEEE Int. Conf. on Robotics and Automation (ICRA)*, 2017.
- [23] N. A. Spielberg, M. Brown, and J. C. Gerdes, "Neural Network Model Predictive Motion Control Applied to Automated Driving With Unknown Friction," *IEEE Trans. on Control Systems Technology*, 2021.
- [24] P. Ventura Diaz and S. Yoon, "High-fidelity computational aerodynamics of multi-rotor unmanned aerial vehicles," in *2018 AIAA Aerospace Sciences Meeting*, 2018.
- [25] R. Verschuere, G. Frison, D. Kouzoupis, J. Frey, N. van Duijkeren, A. Zanelli, B. Novoselnik, T. Albin, R. Quirynen, and M. Diehl, "acados: a modular open-source framework for fast embedded optimal control," *Mathematical Programming Computation*, 2021.
- [26] J. A. E. Andersson, J. Gillis, G. Horn, J. B. Rawlings, and M. Diehl, "CasADi: a software framework for nonlinear optimization and optimal control," *Mathematical Programming Computation*, 2019.
- [27] M. Diehl, H. Bock, J. P. Schlöder, R. Findeisen, Z. Nagy, and F. Allgöwer, "Real-time optimization and nonlinear model predictive control of processes governed by differential-algebraic equations," *Journal of Process Control*, 2002.
- [28] D. Falanga, P. Foehn, P. Lu, and D. Scaramuzza, "PAMPC: Perception-Aware Model Predictive Control for Quadrotors," in *2018 IEEE/RSJ Int. Conf. on Intelligent Robots and Systems (IROS)*, 2018.
- [29] M. Kamel, T. Stastny, K. Alexis, and R. Siegwart, "Model Predictive Control for Trajectory Tracking of Unmanned Aerial Vehicles Using Robot Operating System," in *Robot Operating System (ROS)*, 2017.
- [30] flaticon.com, *This paper has been designed using resources from flaticon.com*.